Organometallics **1990,** *9,* 379–387

Acknowledgment. We thank Professor R. A. Andersen and Dr. C. J. Burns at the University of California, Berkeley, CA, for providing the compounds and Professor A. Haaland at the University of Oslo for helpful discussions. We also thank The Norwegian Research Council for Science and the Humanities and the VISTA program for financial support.

Registry No. I, 112379-48-3; II, 112379-49-4; $Mg(C_5H_5)_2$, 63757-86-8; $Ca(C_5H_5)_2$, 33379-52-1.

Synthesis and NMR Spectroscopy of Cyclopalladated Tertiary Phosphite Complexes. X-ray Crystal Structure of $Pd(\eta^5\text{-}C_5H_5)(P(OPh)_2(OC_6H_4))$

Alberto Albinati*

Istituto di Chimica Farmaceutica, Università di Milano, Viale Abruzzi 42, I-20131 Milano, Italy

Samuel Affolter and Paul S. Pregosin*

Laboratorium für anorganische Chemie, ETH-Z, Universitätstrasse 6, CH-8092 Zürich, Switzerland

Received June 8, 1989

A series of cyclopalladated tertiary phosphite complexes of structure $[Pd(\mu\text{-}Cl)(P(OR^1)_2(OC_6H_3R^2))]_2$ (2), with R^1 being either Ph or Et, has been prepared and studied with use of ^{31}P, ^{13}C, and ^1H NMR methods. For **2a** (R^1 = Ph, R^2 = H) there are two isomers that have been assigned to the sym-cis and sym-trans structures and that are in equilibrium as shown by ^{31}P 2-D exchange NMR spectroscopy. For the platinum analogue of **2a**, the exchange can be shown to be intramolecular, again via 2-D exchange NMR spectroscopy. An analysis of the ^{13}C NMR characteristics for 2 and some mononuclear derivatives obtained with use of PPh_3, $AsPh_3$, $C{\equiv}NBu^t$, diphos, CH_3CN, and $\eta^5\text{-}C_5H_5$ suggests that the low-field shift of the palladated carbon arises from the nature of the Pd–C bond and not a ring effect. Various approaches to the syntheses of 2 are discussed, and cyclopalladation of $P(OEt)_2(NMePh)$ is presented. The molecular structure of $Pd(\eta^5\text{-}C_5H_5)(P(OPh)_2(OC_6H_4))$ has been determined by X-ray diffraction. The complex crystallized in the space group $P2_12_12_1$, with a = 9.197 (4) Å, b = 10.807 (3) Å, c = 20.718 (3) Å, V = 2059 (2) Å^3, and Z = 4. The structure was refined to R = 0.045. Relevant bond distances (Å) and angles (deg) are as follows: Pd–P = 2.150 (2), Pd–C(2) = 2.026 (6), Pd–C(19) = 2.347 (9), Pd–C(20) = 2.301 (7), Pd–C(21) = 2.346 (7), Pd–C(22) = 2.283 (7), Pd–C(23) = 2.300 (7); P–Pd–C(2) = 80.2 (2). The dihedral angle between the P–Pd–C(2) and $\eta^5\text{-}C_5H_5$ planes is 87.1°.

Introduction

Cyclopalladation is now a widely recognized reaction[1] with potential applications for organic synthesis.[2-5] Our interest in the cyclopalladation[6,7] of benzylideneanilines and their eventual conversion to ortho-substituted aldehyde derivatives has prompted us to extend our studies to phenol-related ligands, with specific emphasis on phosphites. There is relatively sparse literature concerned with the cyclometalation of phosphites involving Pd(II) and Pt(II)[8] and also a few Fe(II),[9] Ru(II),[10] Mn(I),[11] and Os(II)[12] derivatives. Normally, for the Pd(II) chemistry, yields were modest and the spectroscopic possibilities limited. We report here our initial studies on the cyclometalation and characterization of complexes derived from $P(OPh)_3$ and $P(OEt)_2(OPh)$, with the latter ligand selected so that after cyclometalation and subsequent transformation (e.g., carbonylation), hydrolysis would readily yield the ortho-

Scheme I

$$cis\text{-}PdCl_2(P(OPh)_3)_2 + Ag(CF_3SO_3) \xrightarrow[-60\,°C]{\text{solvent}}$$

$$AgCl + cis\text{- and } trans\text{-}[PdCl(\text{solvent})(P(OPh)_3)_2]^+CF_3SO_3^-$$

solvent = MeOH, acetone

For MeOH: $\delta(^{31}P)_{cis}$ = 83.1, 70.8, $^2J(P,P)$ = 50 Hz; $\delta(^{31}P)_{trans}$ = 86.8; trans:cis ca. 1:20

for acetone: $\delta(^{31}P)_{cis}$ = 81.8, 72.8, $^2J(P,P)$ = 52 Hz; $\delta(^{31}P)_{trans}$ = 84.4; trans:cis ca. 1:8

---

[1] Dehand, J.; Pfeffer, M. *Coord. Chem. Rev.* **1976**, *18*, 327. Omae, I. *Chem. Rev.* **1979**, *79*, 287.

[2] Maasarani, F.; Pfeffer, M.; Le Borne, G. *Organometallics* **1987**, *6*, 2029, 2043.

[3] Horino, H.; Inoue, H. *J. Org. Chem.* **1981**, *46*, 4416.

[4] Horino, H.; Inoue, N. *Teterahedron Lett.* **1979**, *26*, 2403.

[5] Murahashi, S.; Tamba, Y.; Yamamura, M.; Yoshimura, N. *J. Org. Chem.* **1978**, *43*, 4099.

[6] Pregosin, P. S.; Rüedi, R. *J. Organomet. Chem.* **1984**, *273*, 401.

[7] Albinati, A.; Pregosin, P. S.; Rüedi, R. *Helv. Chim. Acta* **1985**, *68*, 2046.

[8] Ahmad, N.; Ainscough, E. W.; James, T. A.; Robinson, S. D. *J. Chem. Soc., Dalton Trans.* **1973**, 1148, 1151.

[9] Stewart, R. R., Jr.; Isbrandt, L. R.; Benedict, J.; Palmer, J. G. *J. Am. Chem. Soc.* **1976**, *98*, 3215.

[10] Lewis, L. N. *Inorg. Chem.* **1985**, *24*, 4433; *J. Am. Chem. Soc.* **1986**, *108*, 743.

[11] Stewart, R. P., Jr.; Isbrandt, L. R.; Benedikt, J. *Inorg. Chem.* **1976**, *15*, 2011.

[12] Ainscough, E. W.; James, T. A.; Robinson, S. D.; Wingfield, J. N. *J. Chem. Soc., Dalton Trans.* **1974**, 2384.

0276-7333/90/2309-0379$02.50/0 © 1990 American Chemical Society

Chart I. Monodentate and Cyclometalated Phosphite Complexes[a]

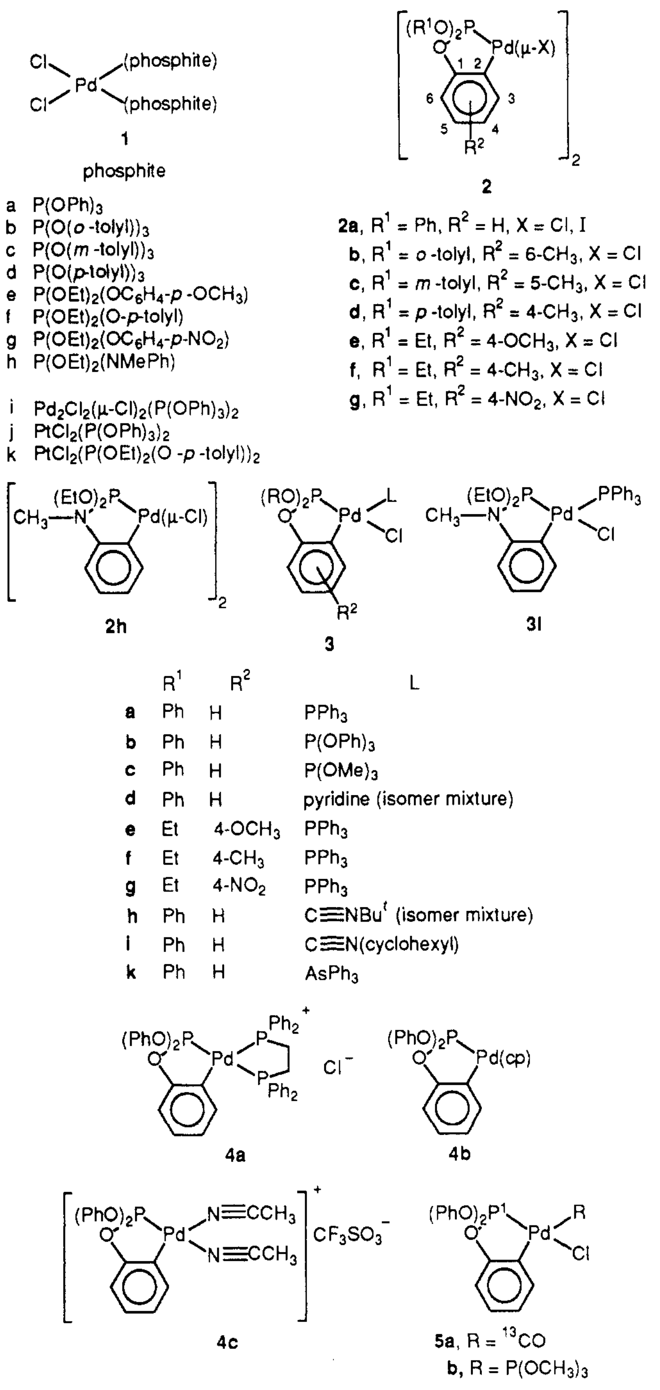

1

phosphite

- a $P(OPh)_3$
- b $P(O(o\text{-tolyl}))_3$
- c $P(O(m\text{-tolyl}))_3$
- d $P(O(p\text{-tolyl}))_3$
- e $P(OEt)_2(OC_6H_4\text{-}p\text{-}OCH_3)$
- f $P(OEt)_2(O\text{-}p\text{-tolyl})$
- g $P(OEt)_2(OC_6H_4\text{-}p\text{-}NO_2)$
- h $P(OEt)_2(NMePh)$

- i $Pd_2Cl_2(\mu\text{-}Cl)_2(P(OPh)_3)_2$
- j $PtCl_2(P(OPh)_3)_2$
- k $PtCl_2(P(OEt)_2(O\text{-}p\text{-tolyl}))_2$

2

2a, R^1 = Ph, R^2 = H, X = Cl, I
b, R^1 = o-tolyl, R^2 = 6-CH_3, X = Cl
c, R^1 = m-tolyl, R^2 = 5-CH_3, X = Cl
d, R^1 = p-tolyl, R^2 = 4-CH_3, X = Cl
e, R^1 = Et, R^2 = 4-OCH_3, X = Cl
f, R^1 = Et, R^2 = 4-CH_3, X = Cl
g, R^1 = Et, R^2 = 4-NO_2, X = Cl

2h 3 3l

	R^1	R^2	L
a	Ph	H	PPh_3
b	Ph	H	$P(OPh)_3$
c	Ph	H	$P(OMe)_3$
d	Ph	H	pyridine (isomer mixture)
e	Et	4-OCH_3	PPh_3
f	Et	4-CH_3	PPh_3
g	Et	4-NO_2	PPh_3
h	Ph	H	$C{\equiv}NBu^t$ (isomer mixture)
i	Ph	H	$C{\equiv}N$(cyclohexyl)
k	Ph	H	$AsPh_3$

4a 4b

4c

5a, R = ^{13}CO
b, R = $P(OCH_3)_3$

[a] I:II for 2a (X = Cl): 65:35, CD_2Cl_2; 75:25, $CDCl_3$; 90:10, C_6D_6.

substituted phenol. For comparison purposes we have also prepared and cyclopalladated $P(OEt)_2(NMePh)$, an N-methylaniline analogue. In the course of this work, the crystal structure of $Pd(\eta^5\text{-}C_5H_5)(P(OPh)_2(OC_6H_4))$ was determined and found to contain some interesting features, which are discussed as well.

Results and Discussion

1. Syntheses. Our initial attempts to prepare cyclometalated phosphite complexes from $Pd(OAc)_2$ in $CDCl_3$ with 1 equiv of $P(OPh)_3$ at room temperature were accompanied by some decomposition. ^{31}P NMR spectroscopy showed a mixture of components, one of which was likely to be the desired complex. A second approach that involved palladium cations, generated as shown in Scheme I, afforded solvent complexes whose structures were likely to be those shown in the scheme on the basis of ^{31}P NMR spectroscopy; however, these solvent complexes are not stable at room temperature.

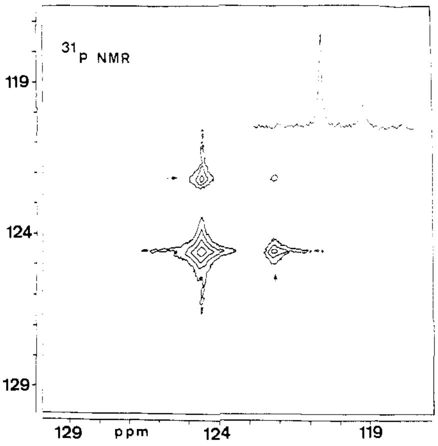

Figure 1. ^{31}P 2-D exchange spectrum for the two isomers of 2a (X = Cl). The appearance of substantial cross peaks (arrows) confirms that the two molecules exchange in solution. The inset (above right) shows the conventional 1-D spectrum (WM-250 spectrometer, $CDCl_3$, room temperature).

Good (ca. 80%) to excellent (essentially quantitative) conversion to the dinuclear complexes $[Pd(\mu\text{-}Cl)(P\frown C)]_2$ (2, $P\frown C$ = cyclopalladated phosphite) was achieved by refluxing the complexes cis-$PdCl_2$(phosphite)$_2$ (1) with 1 equiv of $PdCl_2$ in either toluene or xylene for 1–5 h (see Experimental Section). Previous[8] successes afforded ca. 50% yields, and we attribute our improvement to both the removal of HCl via the use of a slow stream of N_2 during the refluxing period and the choice of a moderate reaction temperature. Analytically pure samples of the complexes 2 react with HCl gas to give dinuclear $[Pd(\mu\text{-}Cl)Cl(\text{phosphite})]_2$. As is typical[1] for cyclometalated complexes with bridging halogens, reactions with 2 equiv of tertiary phosphine or isonitrile, L, afford the mononuclear complexes $PdCl(P\frown C)L$ (3). In a similar fashion, the complexes 4a–c were readily obtained. A list of the various complexes prepared is shown in Chart I. The characterization of the complexes stems from ^{31}P, ^{13}C, and ^1H NMR studies in conjunction with IR and microanalytical data (see Tables I–V). For the $PdCl_2L_2$ (and some $PtCl_2L_2$) complexes the cis geometry could be assigned by using the number and position of M–Cl stretching frequences in the range 269–348 cm^{-1}. For the few platinum complexes 1j, 1k, and 5, ^1J(Pt,P) values helped to make the assignment of geometry,[8,13,14] and this brings us to phosphorus NMR spectroscopy.

2. ^{31}P NMR Spectroscopy. ^{31}P NMR spectra were measured for all of the complexes, and these data, together with the IR M–Cl vibrations, melting points, and isolated yields are shown in Table I. All of the cyclopalladated molecules reveal marked ^{31}P downfield shifts on the order of 40 ppm relative to the signals for the cis-$PdCl_2$(phosphite)$_2$ complexes, thereby providing a useful empirical method for recognizing cyclometalation. For the complexes 3, which contain a second ^{31}P spin, the values ^2J(P,P) (48–56 Hz) are all consistent with cis-phosphorus spins, thereby placing the entering phosphine (or phosphite)

---

(13) Pregosin, P. S.; Kunz, R. W. In *NMR Basic Principles and Progress*; Dieke, P., Fluck, E., Kosfeld, R., Eds.; Springer-Verlag: West Berlin, 1979; Vol. 16.

(14) Pregosin, P. S. In *Methods in Stereochemical Analysis*; Verkade, J. G., Quin, L. D., Eds.; VCH: Weinheim, FRG, 1987; Vol, 8, p 465.

Table I. ^{31}P NMR, IR, and Melting Point Data[a] for the Complexes

complex	color	mp	P1/P2	ν(Pd–Cl)	yield, %
1a (M = Pd)	colorless	174–176	83.0	332, 303	96
1a[b] (M = Pt)	colorless	186–187	58.8	330, 305	98
1b	colorless	175	81.3	330, 299	87
1c	colorless	146	82.4	330, 299	83
1d	colorless	179	83.9	331, 306	80
1e	pale green		90.6	323, 298	86
1f (M = Pd)	colorless	92–93	89.7	327, 300	92
1f[c] (M = Pt)	colorless	137–138	65.0	320, 294	98
1g	pale yellow		88.5	330, 299	92
1h	pale green		94.9	310, 284	89
1i	orange	162 (dec)	55.9[d]	339, 269	49
2a (X = Cl)	pale yellow	170–172	124.6 (I)[e,f] 122.3 (II)	348, 307	79
2a (X = I)	pale yellow	191–192	120.7 (I)[e] 119.5 (II)	343, 307[l]	92
2b	pale yellow	130	122.9 (I)[e] 120.7 (II)		80
2c	pale yellow	186	124.4 (I)[e] 121.6 (II)		79
2d	pale yellow	oil	125.3 (I)[e] 123.1 (II)[e]		100
2e	pale yellow		127.9[e]		90
2f	pale yellow		130.3[e,g]		96
2g	yellow		127.0[e]		97
2h	yellow		131.7[e]		*o*
3a	colorless	184 (dec)	129.9/17.8 (PPh_3) [48][h]	329	96
3b	colorless	142	127.9/108.9 ($P(OPh)_3$) [56][h]	313	99
3c	colorless		133.5/124.5 ($P(OOme)_3$) [55][h]	329	89
3d	colorless	118–119	129.4 (I)[i] 124.4 (II)	308 (I) 283 (II)	94
3e	colorless		134.0/17.2 (PPh_3) [45][h]		90
3f	pale yellow		127.2/16.7 (PPh_3) [47][h]		90
3g	pale yellow		133.6/17.4 (PPh_3) [42][h]		90
3h	colorless	142 (dec)	132.8 (I)[j]	294, 261[j] 2208 (I)[p] 2170 (II)[p]	100
3i	colorless	114–115 (dec)	132.5 (I)[j] 129.2 (II)	306, 278[j] 2223 (I)[p] 2197 (II)[p]	100
3k	colorless	157–158	130.3	322	
3l	pale yellow		140/17.3 (PPh_3) [46][h]		*o*
4a	yellow	155–165	135.8[k]		100
4b	orange	109–110	151.8		72
4c	colorless	oil	125.0 (CD_3CN)		100
5a			105.8	2321, 2294[p] 329[n] 2113[q]	
5b			104.8/28.0 ($P(OCH_3)_3$) [32][h]	321[n]	

[a] Chemical shifts are in ppm (H_3PO_4) and coupling constants in Hz ($CDCl_3$ solutions); ν values are in cm^{-1}; melting points (in °C) are *reproducible*. Decomposition points are noted as dec. [b] ^1J(Pt,P) = 5805 Hz. [c] ^1J(Pt,P) = 5765 Hz. [d] Broad, line width ca. 20 Hz, sharp at 233 K, 56.4 ppm. [e] Broad, line width ca. 20 Hz where isomers I and II are observed; I:II = ca. 70:30. [f] At 233 K, δ = 126.3, 123.4, sharp signals with *no* exchange at 293 K; the 2-D exchange spectrum shows an equilibrium. [g] At 233 K, δ = 131.2 and 131.1 in the ratio ca. 70:30. [h] ^2J(P,P). [i] I:II = ca. 70:30. [j] I:II = ca. 70:30; I = trans C atoms, II = cis C atoms. [k] diphos ^{31}P at δ = 54.8 with ^2J(P,P^1) = 515 Hz trans to phosphite and δ = 44.5 with ^2J(P,P) = 30, 30 Hz (coincidental triplet) cis to phosphite. [l] γ(Pd–I). [m] Not isolated, on the basis of NMR spectroscopy. [n] Pt–Cl stretch. [o] See the Experimental Section. [p] ν(C≡N). [q] ν(CO).

Table II. ^{13}C NMR Data[a] for *cis*-$PdCl_2$(phosphite)$_2$ (1)

compd	C1	C2	C3	C4
1a (M = Pd)	150.7 (8)	121.0 (6)	130.2	126.5
1j (M = Pt)[b]	150.9 (8)	120.9 (5)	130.0	125.8
1f (M = Pd)[c]	148.8 (7)	120.8 (6)	130.4	135.0
1f (M = Pt)[b,d]	149.0 (8)	120.7 (4)	130.3	134.8
1i	150.2 (9)	120.8 (7)	130.8	126.5

[a] In ppm; the value in parentheses is estimated ^nJ(P,C) (in Hz). ^{13}C is the X part of an AA′X spin system ($CDCl_3$, room temperature). [b] ^{195}Pt coupling not observed. [c] CH_2O, 65.4 (2); OCH_2CH_3, 16.1 (7); CH_3, 20.9. [d] CH_2O, 64.9 (7); OCH_2CH_3, 16.0 (7); CH_3, 20.9.

trans to the cyclopalladated carbon. The dinuclear complexes **2a–d** reveal ^{31}P spectra containing two resonances I and II, separated by 1.2–2.8 ppm. For **2a** (X = Cl) these two compounds are in equilibrium, as shown by ^{31}P 2-D exchange spectroscopy (see Figure 1) with the lower field component more abundant. This equilibrium is solvent-dependent (see Chart I) such that nonpolar solvents favor I. The Pt complex analogous to **2a** (X = Cl) also shows two forms that are in equilibrium; however, the two-dimensional ^{31}P exchange spectrum for this material reveals no exchange of the ^{195}Pt isotopomer with that of the magnetically inactive platinum isotopomer, thereby showing the exchange to be *intramolecular*.[15] A detailed analysis of the ^{195}Pt satellites in the ^{31}P spectrum afforded ^2J(Pt,Pt) in addition to the usual ^{31}P parameters (see Scheme II). The substantial difference between the two metal–metal coupling constants 279 and 61 Hz, for I and II, respectively, is consistent with a change in molecular structure, as opposed to a conformational change.[16] Consequently, we assign the sym-trans (I) and sym-cis (II)

---

(15) Rüegger, H.; Pregosin, P. S. *Inorg. Chem.* **1987**, *26*, 2912.
(16) Pregosin, P. S. *Annu. Rep. NMR Spectrosc.* **1986**, *17*, 285.

Table III. ^{13}C NMR Data[a,b] for the Cyclometalated Complexes

complex	C1	C2	C3	C4	C5	C6
2a (X = Cl, I)[c]	155.2 (23.5)	133.6	136.5	123.2	127.8	111.5 (23.5)
2a (X = Cl, II)	155.2 (23.5)	133.5	155.3	123.3	127.8	111.5 (23.5)
2a (X = I)	156.0 (~25)	*e*	142.2	124.2	127.9	111.9 (24)
2f (I)[d]	154 (~20)	130	136.3	133.2	128.4	110.9 (23.5)
2f (II)	156 (~20)			132.4		
3a[f]	155.9 (23.5) [2]	142.4 (2) [120]	137.6 (4.5)	123.8 [7.5]	128.5	111.1 (22) [4]
3b[g]	156.5 (24) [4]	141.9 (0) [190]	137.2 (6) [6]	123.6 (0) [12.5]	128.9	111.1 (22) [7]
3c[h]	157.0 (24.5) [55]	142.5 (0) [182]	136.5 (4.5)	123.6 (0) [12]	128.7	111.2 (22) [7]
3h[i]	157.6 (25.0)	140.5	137.5 (3)	123.7	128.4	111.2 (23.5)
3i[j]	157.6 (25.5)	140.5	137.6 (6)	123.8	128.5	111.3 (24)
3k	156.3 (24.5)	140.7 (52)	137.4	123.8	128.5	111.3 (22.5)
4b[k]	156.7 (25)	134.3 (17.5)	143.8 (4)	122.7	125.7	111.7 (19)
4c[l]	156.1 (22)		135.9 (4)	124.1	129.2	112.2 (24.5)
5a[m]	159.8 (19) {19}	134.5 (85) {815.3}	135.1 (1.5)	123.5 {38.6}	130.0	111.3 (19.4) {11.5}
5b	159.5 (17) [3.7] {29.5}	142.3 (65) [160.4] {718}	135.0	123.2 [10] {33.1}	128.6	110.8 (18.3) [4.8] {13}

[a] In ppm at room temperature in $CDCl_3$; *J* (in Hz) in parentheses refers to P^1, *J* in brackets to L, and *J* in braces to ^{195}Pt. I and II refer to sym-trans and sym-cis isomers, or cis and trans isomers of **3**. [b] The unmetalated $P(OPh)_2$ moiety shows the following ^{13}C signals: C1′, 148.5–150.9; C2′, 120.6–122.1; C3′, 129.8–130.7; C4′, 125.7–127.2. [c] 233 K. [d] 293 K; I:II = ca. 70:30, $\Delta\delta_{1/2} \approx 10$ Hz. Additional bands: CH_2O, 64.8 (11.8); $\mathit{C}H_3CH_2O$, 16.4 (7); CH_3, 21.1. [e] Not observed. [f] PPh_3: 131.8 (40), 135.0 (12), 128.7 (10), 130.0. [g] $P(OPh)_3$: 150.8 (6), 121.3 (5), 130.1, 125.7. [h] $\mathit{C}H_3O$, 52.5. [i] Major isomer, isonitrile trans to carbon. Cyclohexyl bands: 54.7, 32.2, 24.9, 23.1. [j] Major isomer, isonitrile trans to carbon, Bu^t bands: 58.1 and 30.1. [k] cp: 96.9 (3.5). [l] Additional bands: $\mathit{C}H_3CN$, 2.6; $CH_3\mathit{C}N$, broad ca. 119.2; $\mathit{C}F_3SO_3^-$, 120.5 (J(C,F) = 320 Hz). [m] $\delta(\mathit{C}O)$ = 176.8, ^1J(Pt,C) = 950 Hz, ^2J(P1,C) = 8.7 Hz.

Table IV. ^{1}H NMR Data[a,b] for Selected Complexes

complex[c]	H3[d]	H5[d]	H6[d]	comments
2e	7.15	6.64[f]	6.77[f]	CH_3O, 3.78; CH_2O, 4.40; OCH_2CH_3, 1.43
2f[e]	7.46 (7)	6.90[f]	6.73[f]	CH_3, 2.28 (I), 2.31 (II)
	7.73 (7)			CH_2O, 4.42; OCH_2CH_3, 1.43
2g[e]	8.39 (5)	8.03	6.95	CH_2O, 4.45; OCH_2CH_3, 1.46
	8.20	8.14	6.94	
2h	7.72 (7)	7.07	6.38	CH_3N, 2.81 ($J(P^1)$ = 8); H4, 6.72
3e	8.08 (5.6) [8.5]	6.67 (2.5)	6.77 (0) [4.0]	CH_3O, 3.84; CH_2O, 3.87
3f	8.22 (5.8) [7.3]	6.93 (1.5)	6.75 (0) [3.5]	CH_3, 2.32; CH_2O, 3.90
3g	9.31 (4.9) [8.0]	8.02 (2.3)	6.93 (0) [3.3]	CH_2O, 3.92
3l	8.61 (4.7) [7.7]	7.14 (3.1)	6.45 (0) [3.4]	CH_2O, 3.80; H4, 6.90 (3) [2.9]
4b	7.59 (2.0)	7.05 (1.5)	6.99	cp,5.45 ($J(P^1)$ = 2.5 Hz); H4, 6.79

[a] In $CDCl_3$ at room temperature, with values in ppm. The complexes **1** show (1) unresolved or poorly resolved aromatic resonances often of the AA′BB type, (2) CH_3 resonances for **1b** (2.09), **1c** (2.25), **1d** (2.33), **1f** (M = Pd) (2.33), **1f** (M = Pt) and (2.30) **1h** (3.18), and (3) bands for the OCH_2CH_3 group, $OCH_2\mathit{CH}_3$ at ca. 1.18–135 and $O\mathit{CH}_2$ at ca. 4.3. This OCH_2 group often shows nonequivalent protons: **1f** (M = Pd), δ 4.30, 4.32, ^2J(H,H) = 7.5 Hz; **1h**, δ 3.97, 4.09, ^2J(H,H) = 10.0 Hz. [b] Additional bands: **2b**, CH_3 at 2.34; **2c**, CH_3 at 2.29 (6), 2.03 (3); **2d**, CH_3 at 2.28 (6), 2.21 (3); **3a**, H3 at 8.45 (5.5), 7.5; **3b**, H3 at 8.20 (5.5), 13.0; **3c**, H3 at 8.23 (5.5), 13.0, **3i**, isomer I, H3 at 8.24 (7.5). [c] Certain ^nJ(H,H) values are general: ^3J(H,H)(aromatics) = 8–9 Hz; ^4J(H,H)(aromatics) = 1.5–3 Hz; $^3J(O\mathit{CH}_2\mathit{CH}_3)$ = ca. 7 Hz. [d] *J* values in Hz: in parentheses, coupling to P1; in brackets, coupling to P2. For **3k** ($AsPh_3$ complex) δ (H3) = 8.43 and J(P,H) = 5.8 Hz. [e] The first value refers to isomer I and the second to isomer II; I:II = 70:30. [f] Tentative assignments.

Table V. Analytical Data for Selected Compounds

	anal. calcd (found), %		
compd	C	H	Cl
1e (M = Pd)	39.69 (39.14)	5.15 (5.20)	10.65 (10.62)
1f (M = Pd)	41.67 (41.63)	5.37 (5.69)	11.22 (11.18)
1f (M = Pt)	36.59 (36.14)	4.74 (4.63)	9.81 (10.02)
2a (X = Cl)[a]	47.92 (47.91)	3.13 (3.14)	7.86 (8.22)
2a (X = I)	39.84 (39.88)	2.60 (2.60)	
2b	51.14 (51.39)	4.09 (4.18)	7.19 (7.38)
2c	51.14 (51.10)	4.09 (4.03)	7.19 (7.02)
2e	34.31 (34.36)	4.19 (4.35)	9.21 (9.13)
3a	60.21 (60.25)	4.10 (4.16)	4.97 (5.02)
3c	43.85 (43.44)	4.03 (3.96)	6.16 (6.31)
3d	52.10 (52.21)	3.61 (3.43)	6.69 (6.59)
3h[b]	51.70 (51.60)	4.35 (4.53)	6.64 (6.75)
3i[c]	53.59 (53.37)	4.50 (4.64)	6.33 (6.53)
3k	57.09 (56.90)	3.86 (3.76)	4.68 (4.71)
4a[d]	62.21 (61.27)	4.51 (4.78)	4.17 (4.55)
4b[e]	57.46 (57.22)	3.98 (4.04)	4.68 (4.71)
5a	40.17 (40.28)	2.47 (2.38)	6.25 (6.16)
5b	37.97 (37.79)	3.47 (3.50)	5.34 (5.30)
6[f]	40.05 (40.45)	2.61 (2.57)	6.57 (6.38)

[a] M_r = 900.3 (905.5). [b] % N 2.62 (2.64). [c] % N 2.50 (2.48). [d] Contains solvent. [e] M_r = 480.4 (477.9). [f] $[Pt(\mu\text{-}Cl)(P(OPh)_2(OC_6H_4))]_2$.

structures to these molecules and tentatively[59] suggest that the isomerization proceeds via bridge splitting and isomerization of the three-coordinate species that arises, followed by recombination. We assume that the palladium analogues are isomerizing in a similar way. We note that $[Pt(\mu\text{-}OH)ClL]_2$[17] (L = PEt_3, PMe_2Ph, PEt_2Ph) [Pt(μ-

Scheme II

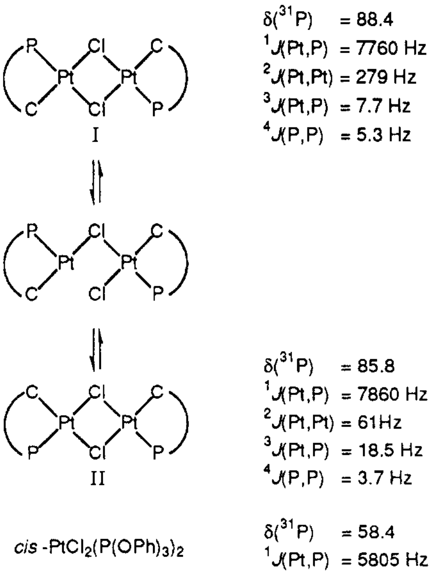

Cl)Ph(PMePh$_2$)]$_2$ and [Pt(μ-Cl)(acyl)(PMePh$_2$)]$_2$[19] have been suggested to exist in sym-trans and sym-cis forms in solution.

3. ^{13}C NMR Spectroscopy. Carbon-13 NMR spectroscopy is a valuable method for detecting cyclometalation in that (1) the symmetry of the metalated ring is often lower and (2) an additional nonprotonated ^{13}C signal is readily detected. Despite a number of reports[6,20,23] containing ^{13}C data for cyclometalated complexes, the position of the Pd–C(aryl) carbon is occasionally uncertain[20,22] and is often unexplained. In our complexes, as well as in those of cyclopalladated nitrogen and phosphorus ligands, the metalated carbon appears downfield relative to an analogous protonated carbon, frequently by some 10–30 ppm. There are at least four factors that can be expected to make substantial contributions to the shielding of the Pd–C carbon resonance position: (1) substituents on the cyclopalladated moiety; (2) the cis and trans influences of ligands, i.e., effects from the ligands transmitted via the metal; (3) a "ring effect" as in ^{31}P NMR spectroscopy[24] (4) electronic perturbations due to the metal itself, i.e., the change ^{13}C–H $\rightarrow$ ^{13}C–ML$_n$.

We have already discussed point 1 in connection with the cyclopalladation of benzylideneanilines[6] and shown that, for para substitution, normal aromatic substituent effects are found; i.e., there is no marked change in the resonance and inductive effects due to the presence of palladium. Consequently, relative to the signals for other cyclopalladated complexes we expect an upfield shift of our palladated carbon due to the donor substituent effect of the phosphite oxygens. We estimate the magnitude of this effect at 7–8 ppm (relative to C_6H_6) on the basis of δ(C2) for the bis(phosphite) complexes 1 (table II). In addition we note that δ(C2) for uncoordinated P(OPh)$_3$ is 121.0 ppm. It is also known, especially in the chemistry of Pt(II), that the trans ligand markedly effects δ^{13}C(aryl)) such that stronger donors induce a *low*-field shift.[25] For the cations PtPhL(AsMe$_3$)$_2^+$ the change may be as much as ca. 26 ppm,[25] between L = DMF and a cyclic carbene.[25]

We are inclined to attribute only minor importance to a potential "ring effect" arising from a five-membered ring since the observed downfield shifts in six-membered rings are comparable[26,27] and the effects of metalation, in the absence of a ring, are as large, or larger, than $\Delta\delta$ due to cyclometalation (see Chart II). Consequently, the low-field shift on metalation[60] is electronic in origin and is presumably related to the energy of the M–C lone pair in relation to that of the remaining LUMO's in the molecule. We note that phenyllithium shows δ(C1) in the range 171.7[28] to 188.7 ppm.[29] Returning to our complexes **2**–**4**, we find low-field shifts on metalation of ca. 9–22 ppm, with the larger values arising, as expected, for the complexes **3** with phosphorus trans to carbon. These $\Delta\delta$ values are modest

Chart II. ^{13}C Data for Model and Palladated Complexes[a]

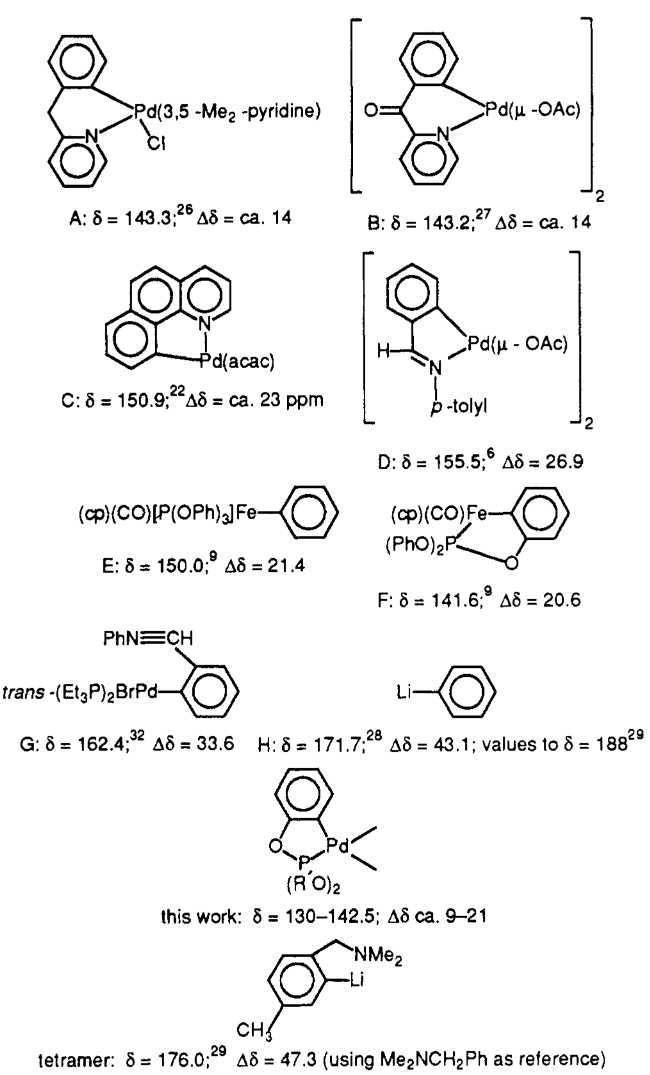

[a] δ is for the *metalated carbon only*. In some cases the literature assignments are uncertain; however, these errors do not affect the qualitative nature of these arguments. $\delta(C_6H_6)$ = 128.6; δ(C2) for P(OPh)$_3$ = 121.0.

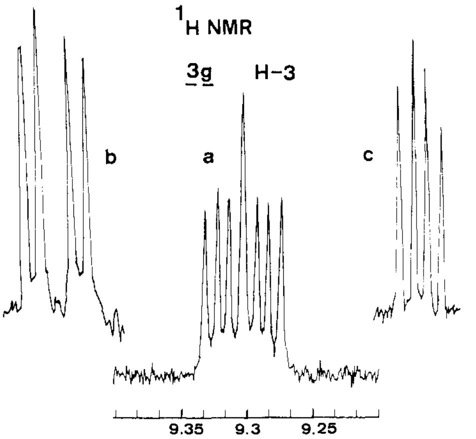

Figure 2. ^{1}H NMR spectra of H3 in complex **3g**: (a) conventional spectrum showing splittings arising from three spins; (b) spectrum with phosphte ^{31}P decoupling; (c) spectrum with PPh$_3$ ^{31}P decoupling (WM-250 spectrometer, CDCl$_3$). ^3J(H3,H5) = 2.7 Hz, ^4J(P(phosphine),H3) = 8.0 Hz, and ^4J(P(phosphite),H3) = 4.9 Hz.

---

(17) Fakley, M. E.; Pidcock, A. *J. Chem. Soc., Dalton Trans.* **1977**, 1444.

(18) Eaborn, C.; Odell, K. J.; Pidcock, A. *J. Chem. Soc., Dalton Trans.* **1978**, 1288.

(19) Anderson, G. K.; Cross, R. J.; Muir, L. M.; Muir, K. W.; Solomun, T. *J. Organomet. Chem.* **1979**, *170*, 385.

(20) Steel, P. J.; Caygill, G. B. *J. Organomet. Chem.* **1987**, *327*, 101.

(21) Barr, N.; Dyke, S. F.; Frost, R. L. W. *Org. Magn. Reson.* **1984**, *22*, 277.

(22) Garber, A. R.; Garrou, P. E.; Smas, M. J.; Wilkinson, J. R.; Todd, L. J. *J. Organomet. Chem.* **1975**, *86*, 219.

(23) Hiraki, K.; Fuchita, Y.; Takakura, S. *J. Organomet. Chem.* **1981**, *210*, 273.

(24) Garrou, P. E. *Chem. Rev.* **1981**, *81*, 229.

(25) Clark, H. C.; Ward, J. E. H. *J. Am. Chem. Soc.* **1974**, *96*, 1741.

(26) Hiraki, K.; Fuchita, Y.; Takechi, K. *Inorg. Chem.* **1981**, *20*, 4316.

(27) Fuchita, Y.; Hiraki, K.; Klage, Y. *Bull. Chem. Soc. Jpn.* **1982**, *55*, 955.

(28) Mann, B. E.; Taylor, B. F. *^{13}C NMR Data for Organometallic Compounds*; Academic Press: London, 1981.

(29) Wehman, E. Ph.D. Thesis, Univeristy of Amsterdam, 1988.

compared to those of ca. 38 ppm found for some cyclopalladated 1-(phenylazo)naphthalenes[30] and of ca. 50 ppm found in cyclometalated manganese(I) derivatives.[31] Monodentate aryl carbons in *trans*-$PdX(C_6H_4(CH{=}NPh))L_2$ (L = PEt_3, PPh_3; X = halogen) have the Pd–C signal at δ ca. 155–170.[32]

4. ^1H NMR Spectroscopy. The ^1H NMR spectra for the cyclometalated derivatives are also useful in that they show that one hydrogen is no longer present as a consequence of cyclopalladation. Tables IV and V contain an extensive collection of data for both ligands and complexes. As a consequence of the dynamics for **2**, proton H3 is often broad. There are two noteworthy points in connection with these measurements: First, for the complexes **3**, both the phosphite and phosphine ^{31}P spins couple through four bonds to H3, the proton adjacent to the Pd–C bond, as shown by $^1H\{^{31}P\}$ selective decoupling (see Figure 2). Second, this same proton experiences marked local anisotropic effects arising from the ligand cis to the Pd–C bond. This latter point has been recognized by several authors,[33-37] including ourselves.[38] Consequently, as shown in the figure, H3 for **3g** appears at δ ca. 9.3 as a consequence of the deshielding effect of the cis Cl and not due to special electronic effects associated with cyclopalladation. PPh_3 and aromatic nitrogen ligands often induce marked *upfield* shifts in H3, in related cyclopalladated complexes.[33-38]

Interestingly, we have determined a few selective ^5J(P,H5) values, e.g., from the phosphite P^1 in **3e–g** and **3k**, with values of 2–3 Hz. We do *not* observe an analogous $^6J(P^2,H5)$ value arising from P^2 of an L ligand; however, there are 2–4-Hz $^5J(P^2,H)$ values due to coupling of P^2 with H4 and H6.

5. NMR Spectroscopy and Complexes 5. The NMR empiricisms developed in sections 2–4 can now be employed for the CO and $P(OCH_3)_3$ complexes **5**, together with ^1J(Pt,L) (L having suitable spin). The combined data may be analyzed as follows.

Relative to *cis*-$PtCl_2(phosphite)_2$, $\delta(^{31}P)$ values for the complexes **5** appear at 105.8 and 104.8 ppm, almost 50 ppm downfield.

^2J(P,P) and ^2J(P,C) values define the relative orientations of the phosphorus and carbon spins within the molecules; e.g., in **5a** the two C atoms are trans and in **5b** the two P atoms are cis (^2J(P2,C2) = 160.4 Hz in **5b**; remember ^2J(trans) > ^2J(cis)).[13]

The ^1J(Pt,P) and ^1J(Pt,C) values support these findings, based on known trans-influence ideas; e.g., in **5a** ^1J(*Pt,CO*), at 950 Hz, is relatively *small* for a coordinated CO[13,28] and ^1J(Pt,C2) = 815 and 718 Hz in **5a** and **5b**, respectively, are moderate.

The metalated carbons C2 (134.6 ppm, **5a**; 142.3 ppm, **5b**) are at low field relative to C2 in **1**, with the carbon trans to $P(OCH_3)_3$ at lower field due to the difference in trans influence between CO and $P(OCH_3)_3$.

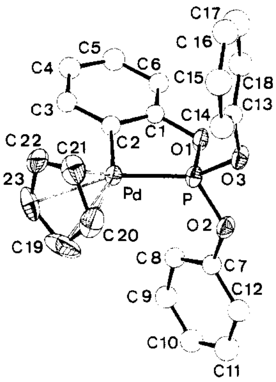

Figure 3. ORTEP plot of **4b**.

Table VI. Selected Bond Lengths (Å) and Bond Angles (deg) for 4b

Pd–P	2.149 (2)	P–O2	1.596 (4)
Pd–C2	2.026 (6)	P–O3	1.599 (4)
Pd–C19	2.351 (9)	C19–C20	1.42 (1)
Pd–C20	2.299 (7)	C20–C21	1.39 (1)
Pd–C21	2.347 (7)	C21–C22	1.36 (1)
Pd–C22	2.283 (7)	C22–C23	1.34 (1)
Pd–C23	2.300 (7)	C19–C23	1.40 (1)
P–O1	1.607 (5)		
P–Pd–C2	80.2 (2)	C19–C20–C21	109.4 (9)
Pd–P–O1	108.4 (2)	C19–C23–C22	109.5 (9)
Pd–P–O2	125.5 (2)	C20–C21–C22	106.1 (8)
Pd–P–O3	122.1 (2)	C21–C22–C23	111.0 (8)
Pd–C2–C1	119.4 (5)	C20–C19–C23	103.8 (7)
Pd–C2–C3	123.4 (5)		

The proton H3, immediately adjacent to Pt, is shifted somewhat downfield, 8.16 and 8.22 ppm, respectively, due in part to the anisotropic effect of the cis-Cl ligand. There are ^4J(P,H) values to both the cyclic ^{31}P (2.0 and 1.8 Hz, respectively) and $P(OCH_3)_3$ (9.2 Hz); ^3J(Pt,H) = 48 and 40 Hz. The combined use of these various NMR probes facilitates recognition of cyclometalation and focuses our understanding since the source of these chemical shifts is somewhat clearer.

6. Molecular Structure of 4b. In view of our interest in phosphite cyclometalation chemistry, we have determined the structure of the η^5-C_5H_5 derivative **4b** by X-ray diffraction methods, and Figure 3 shows an ORTEP view of this molecule. The bond distances within the coordination sphere are normal; the Pd–C2 separation of 2.026 (6) Å is longer than those observed in either the $[Pd(\mu\text{-}Cl)Cl(2\text{-}CH_2\text{-}6\text{-}NO_2C_6H_3)]_2^-$ anion[39] (1.958 (8) Å) or (*N,N*-dimethylbenzylamine-*C,N*)(*N*-phenylsalicylaldiminato)palladium(II)[40] (1.981 (7) Å) but comparable to those found in $Pd(2\text{-}NO_2C_6H_4)_2$ (2.028 (3) and 2.039 (4)Å), a molecule with two *o*-nitrophenyl ligands.[41] The complex $Pd(\eta^5\text{-}C_5H_5)(\eta^1\text{-}C_5H_5)(PPr^i{}_3)$[42] (**6**), with a similar coordination sphere, reveals a Pd–C distance (in the η^1-cp group) of 2.130 (7) Å; however, this carbon ligand has a formally sp^3 Pd–C bond. Our Pd–P distance, 2.150 (2) Å, is shorter than (1) the Pd–P bond length in the η^1-C_5H_5 complex **6** (2.241 (3) Å), (2) those in $[Pd(\eta^5\text{-}C_5H_5)(diphos)](CF_3SO_3)$[43]

---

[30] Klaus, A. J.; Rys, P. *Helv. Chim. Acta* **1981**, *64*, 1452.

[31] Ceder, R. M.; Sales, J.; Solans, X.; Font-Altaba, M. *J. Chem. Soc., Dalton Trans.* **1986**, 1351.

[32] Granell, J.; Sainz, D.; Sales, J.; Solans, X.; Font-Altaba, M. *J. Chem. Soc., Dalton Trans.* **1986**, 1785. Granell, J.; Sales, J.; Villarasa, J.; Declerq, J. P.; Germain, G.; Miravitles, C.; Solans, X. *J. Chem. Soc., Dalton Trans.* **1983**, 2441.

[33] Deeming, A. J.; Meah, M. N.; Bates, P. A.; Hursthouse, M. *J. Chem. Soc., Dalton Trans.* **1988**, 2193.

[34] Hiraki, K.; Fuchita, Y.; Kage, Y. *J. Chem. Soc., Dalton Trans.* **1984**, 99.

[35] Komatsu, T.; Nonoyama, M. *J. Inorg. Nucl. Chem.* **1977**, *39*, 1161.

[36] Ryabov, A. *Inorg. Chem.* **1987**, *26*, 1252.

[37] Polyakov, V. A.; Ryabov, A. D. *J. Chem. Soc., Dalton Trans.* **1986**, 589.

[38] Pregosin, P. S.; Rüedi, R.; Anklin, C. *Magn. Reson. Chem.* **1986**, *24*, 255.

[39] Vicente, J.; Arcas, A.; Borrachero, M. V.; Hursthouse, M. B. *J. Chem. Soc., Dalton Trans.* **1987**, 1655.

[40] Fallon, G. D.; Gatehouse, B. M. *J. Chem. Soc., Dalton Trans.* **1974**, 1632.

[41] Vicente, J.; Chicote, M. T.; Martin, J.; Artigao, M.; Solans, X.; Font-Alba, M.; Aguilo, M. *J. Chem. Soc., Dalton Trans.* **1988**, 141.

[42] Werner, H.; Kraus, H. J.; Schubert, U.; Ackermann, K.; Hofmann, P. *J. Organomet. Chem.* **1983**, *250*, 517.

[43] Bachechi, F.; Lehman, R.; Venanzi, L. M. *J. Crystallogr. Spectrosc. Res.* **1988**.

(2.250 (2) and 2.266 (3) Å), and (3) those for $PdCl_2(PP)$ (PP = (diphenylphosphino)methane, 1,2-(diphenylphosphino)ethane, and 1,3-(diphenylphosphino)propane;[44] all ca. 2.24 Å); however, M–P distances in coordinated phosphorus ligands attached to electron-withdrawing groups are expected to be shorter.[45,46] Specifically, for *cis*-$PtCl_2(PEt_3)(P(OPh)_3)$, the phosphine and phosphite Pt–P separations are 2.268 (1) and 2.182 (2) Å, respectively.[47] Our P–Pd–C(2) angle of ca. 81° is as expected for a five-membered ring,[7,39,41] and the η^5-C_5H_5 plane makes an angle of 87° with the plane defined by P, Pd, and C2. Additional bond separations and bond angles can be found in Table VI.

Pd–C(ring) separations vary over the range 2.284 (7)–2.347 (9) Å and are thus significantly different. Similar differences are found in $Pd(\eta^5\text{-}C_5H_5)(\eta^1\text{-}C_5H_5)(PPr^i_3)$ (**6**)[42] and $[Pd(\eta^5\text{-}C_5H_5)(diphos)](CF_3SO_3)$.[43] Interestingly, in the former, Werner et al.[42] account for these distances using EHT-MO calculations and propose that one of the carbons is coordinated more strongly than the other. Our data confirm this point, since we find a relatively short Pd–C22 separation of 2.284 (7) Å. However, complex **6** shows conformer **7** in the solid state, a fact that is considered important in the calculations, whereas **4b** has conformation **8**, as judged by the P–Pd–C plane, which passes through ring separations C22–C23 and almost eclipses C20. Recently, Anderson et al.[48] have reported the structure of $Pd(cp)(C_6H_4\text{-}2\text{-}N{=}NPh)(P(cy)_3)$ (**9**), a molecule with a coordination sphere similar to that of **6** (η^5-cp, η^1-C, and PR_3), and these authors also find conformer **8**. Their P–Pd–C plane bisects the ring C–C bond containing the shortest Pd–C separation, 2.303 (6) Å (range of C–C separations 2.303 (6)–2.385 (6) Å), as in **4b**. It would seem as if the conformation (**7** or **8**) is not important for the establishment of one short Pd–C distance. Indeed, it has been shown that such rotamers should have very similar energies.[42] Moreover, in neither **4b** nor **9** does one observe the pattern of C–C ring separations found in **6**, although these separations can vary significantly: 1.33–1.43 Å in **4b**, 1.37–1.42 Å in **6**, and 1.354–1.427 Å in **9**. It is reasonable that, despite structural differences in **4b**, **6**, and **9**, the observation of one relatively short Pd–C(ring) distance reflects a common characteristic of their electronic structures. Whether the calculations of Werner et al. on $Pd(cp)(CH_3)(PH_3)$ correctly reflect this electronic factor remains open in our eyes.

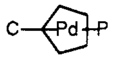

7

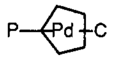

8

Experimental Section

Materials. $PdCl_2$ and $PtCl_2$ were available from Johnson Matthey $AgCF_3SO_3$ and $P(OPh)_3$ from Fluka AG; $Pd(OAc)_2$,[49] $PtCl_2(PhCH{=}CH_2)_2$,[50] and Tl(cp)[51] were prepared via literature methods. Solvents, and especially the isomer mixture of xylenes (bp 136–140 °C), were from Fluka AG and were dried before use. $P(OEt)_2(OPh)$ was prepared from $P(OEt)_2(NEt_2)$[52] as described,[53] and $P(OC_6H_4X)_3$ was made by the method of Walsh.[54] NMR measurements were performed on WM-250 and AM-200 NMR spectrometers in $CDCl_3$ solutions unless otherwise specified. $^1H\{^{31}P\}$ spectra were obtained with use of a ^1H probe head built with a ^{31}P decoupling coil. The ^{31}P frequency was amplified by using a wide-band amplifier before being passed to the probe head. 2-D exchange (NOESY) spectra were measured with use of a conventional pulse sequence[55] with a 0.3-s mixing time.

In Situ Generation of $PtCl(solvent)(P(OPh_3))_2^+$ Cations. Solid *cis*-$PdCl_2(P(OPh)_3)_2$ (39.9 mg, 0.10 mmol) and solid $Ag(CF_3SO_3)$ (12.9 mg, 0.05 mmol) were added to a precooled (−60 °C) solvent mixture composed of either 0.5 mL of acetone-d_6 and 1.0 mL acetone or 0.5 mL of CD_3OD and 1 mL of CH_2Cl_2. Removal of the precipitated AgCl after 0.5 h was followed by ^{31}P measurements at −60 °C.

***cis*-$PdCl_2(P(OPh)_2)_2$ (1a).** $PdCl_2(PhCN)_2$ (384 mg, 1.0 mmol) was dissolved in 15 mL of CH_2Cl_2 and then treated with $P(OPh)_3$ (540 μL, 2.06 mmol). After it was stirred for ca. 10 min, the colorless solution was treated with 65 mL of pentane. The product that precipitated was filtered, washed with pentane, and dried in vacuo; yield 766 mg (96%).

Complexes **1b** and **1d** were prepared analogously. For **1c** and **1h**, the reaction solution was concentrated to afford an oil, which was then suspended in pentane and stirred overnight. Decantation followed by drying in vacuo, afforded the product as a powder. Complex **1h** slowly decomposes, as evidenced by the odor of (presumably) *N*-methylaniline. Complexes **1a–d** have been previously prepared with use of Na_2PdCl_4 in ethanol.

$[Pd(\mu\text{-}Cl)(P(OR^1)_2(OC_6H_3R^2))]_2$ (2a–h). cis-$PdCl_2$(phosphite)$_2$ (0.5 mmol) was dissolved in a suitable high-boiling aromatic solvent (see Table IX) and then treated with $PdCl_2$ (93 mg, 0.53 mmol). The suspension was then refluxed under a slow stream of nitrogen until all the $PdCl_2$ had dissolved and no further HCl was determined in the exit gases. Filtration through Celite, removal of the solvent in vacuo and drying afforded the crude product. The solvents, reaction times, workups, and yields are shown individually for **2a–h** (Table IX). The iodo analogue of **2a** was prepared by metathesis of **2a** (90 mg, 0.10 mmol) with NaI (100 mg, 0.6 mmol) in 2 mL of acetone. The resulting suspension was concentrated and extracted with CH_2Cl_2, the extracts were concentrated once again, and the product was recrystallized from CH_2Cl_2/pentane to afford 103 mg (95%) of product.

$PdCl(P(OPh)_2(OC_6H_4))(PPh_3)$. Complex **2a** (90 mg, 0.70 mmol) was treated with PPh_3 (53 mg, 0.20 mmol) in 2 mL of CH_2Cl_2. After the mixture was stirred for 10 min, the solvent was removed in vacuo and the product recrystallized from CH_2Cl_2/pentane; yield 137 mg (96%). Complexes **3b** and **3c** were prepared analogously. Complexes **3e–g** and **3k** were oily after solvent removal but solidified when suspended in pentane. **3d**, from **2a** (45 mg, 0.05 mmol) and 2 mL of pyridine, was found to be analytically pure after removal of all volatile material (50 mg, 94%); however, recrystallization from CH_2Cl_2/pentane results in some pyridine loss and consequently in a mixture of **2a** and **3d**.

Complex **4a** arises quantitatively from **2a** (90 mg, 0.10 mmol) and diphos (80 mg, 0.20 mmol) in 1 mL of $CDCl_3$ and can be precipitated with pentane.

$Pd(cp)(P(OPh)_2(OC_6H_4))$ (4b). Complex **2a** (156 mg, 0.173 mmol) was dissolved in 6 mL of THF and then treated with Tl(cp) (0.349 mmol). Stirring for 16 h was followed by concentration in vacuo. The crude product was chromatographed by using silica gel with CH_2Cl_2/pentane as eluent. The orange fraction collected could be recrystallized from pentane after removal of the eluent; yield 119 mg (72%).

$[Pt(\mu\text{-}Cl)(P(OPh)_2(OC_6H_4))]_2$. $PtCl_2(P(OPh)_3)_2$ (433 mg, 0.50 mmol) and $PtCl_2$ (140 mg, 0.53 mmol) were refluxed for 9 h in

---

[44] Steffen, W.; Palenik, G. J. *Inorg. Chem.* **1976**, *15*, 2432.

[45] Cotton, F. A.; Darensbourg, D. J.; Klein, S.; Kolthammer, B. W. S. *Inorg. Chem.* **1982**, *21*, 294. Cotton, F. A.; Darensbourg, D. J.; Fisley, W. H. *Inorg. Chem.* **1982**, *20*, 578.

[46] Hitchcock, P. B.; Jacobson, B.; Pidcock, A. *J. Chem. Soc., Dalton Trans.* **1977**, 2032.

[47] Caldwell, A. N.; Muir, L. M.; Muir, K. W. *J. Chem. Soc., Dalton Trans.* **1977**, 2265.

[48] Anderson, G.; Cross, R. J.; Muir, L. M.; Muir, K. W.; Rocamora, M. *Organometallics* **1988**, *7*, 1520.

[49] Henry, P. M. *Palladium Catalysed Oxidation of Hydrocarbons*; D. Reidel: Dordrecht, The Netherlands, 1980; p 7.

[50] Albinati, A.; Caseri, W.; Pregosin, P. S. *Organometallics* **1987**, *6*, 788.

[51] Meister, H. Z. *Angew. Chem.* **1957**, *69*, 533.

[52] *Houben-Weyl Methoden der Organischen Chemie*, 4th ed.; Georg Thieme Verlag: Stuttgart, FRG, 1965; Vol. XII, No. 2 (Organische Phosphorverbindungen), p 99.

[53] Reference 52, pp 62, 72.

[54] Walsh, E. N. *J. Am. Chem. Soc.* **1959**, *81*, 3023.

[55] Hull, W. E. In *Two-Dimensional NMR Spectroscopy*; Croasmum, W. R., Carlson, R. M. K., Eds.; VCH: Weinheim, FRG, 1987; p 67.

Table VII. Crystallographic Parameters and Experimental Data for the X-ray Diffraction Study of Compound 4b[a]

formula	$C_{23}H_{19}O_3PPd$
mol wt	480.78
crystal dimens, mm	0.4 × 0.5 × 0.2
cryst syst	orthorhombic
space group	$P2_12_12_1$
a, Å	9.197 (4)
b, Å	10.807 (3)
c, Å	20.718 (3)
V, Å^3	2059 (2)
Z	4
ρ(calcd), g cm^{-3}	1.551
μ, cm^{-1}	9.84
radiation	Mo K$\bar{\alpha}$ (graphite monochromated: λ = 0.71069 Å)
measd rflns	$+h,+k,+l$
θ range, deg	$2.2 \leq \theta \leq 25.0$
scan type	$\omega/2\theta$
scan width, deg	1.2 + 0.35 tan θ
max counting time, s	65
bkgd time, s	0.5 × scan time
max scan speed, deg min^{-1}	10.2
prescan rejection limit	0.5 (2σ)
prescan acceptance limit	0.03 (33σ)
horiz receiving slit, mm	1.80 + tan θ
vert receiving slit, mm	4.0
no. of obsd data	2067
no. of indept data ($\lvert F^2\rvert_{obs} \geq 2.5\sigma\lvert F\rvert^2$)	1790
no. of params refined	163
R^b	0.045
$R_w{}^c$	0.059

[a] Data collected at room temperature. [b] $R = \sum[\lvert F_o\rvert - 1/k\lvert F_c\rvert]/\sum\lvert F_o\rvert$ for observed reflections. [c] $R_w = [\sum w(\lvert F_o\rvert - 1/k\lvert F_c\rvert)^2/\sum F_o{}^2]^{1/2}$.

100 mL of xylene under an N_2 atomosphere. The solution was filtered hot through Celite and xylene removed. The crude material that results was washed with 20 mL of hexane and dried in vacuo to afford 452 mg (84%) of product. Complexes **5a** and **5b** were prepared by treating this material with 2 equiv of ligand (one ligand per Pt) in CH_2Cl_2.

X-ray Measurements. Crystal Structure of 4b. Crystals suitable for X-ray diffraction were obtained by slow evaporation from hexane and are air stable. A prismatic crystal was chosen and mounted on a glass fiber at a random orientation. The determination of the lattice parameters and space group and data collection were carried out on a Nonius CAD4 diffractometer. The unit cell dimensions were obtained by a least-squares fit of the 2θ values of 25 high-order reflections ($21.0 \leq 2\theta \leq 28.0$) with use of the CAD4 centering routines.[56] From systematic absences the space group was unambiguously determined as $P2_12_12_1$. Crystallographic and other relevant parameters for data collection are listed in Table VII. Data were collected with variable scan speed to obtain constant statistical precision on the measured intensities. Three standard relfections ($\bar{1}21$; $\bar{3}18$; $42\bar{1}$) were measured every 1 h to check the stability of the crystal. No significant variation was detected. The orientation of the crystal was monitored by measuring three standards every 300 reflections. Data have been corrected for Lorentz and polarization factors;[56] an empirical absorption correction was applied by using azimuthal (ψ) scans of three reflections ($84.8 \leq \chi \leq 89.3°$). Transmission factors were in the range 0.738–0.997.

The standard deviations on intensities were calculated in terms of statistics alone, while those on F_o were calculated according to $\sigma(F_o) = [\sigma^2(F_o{}^2) + p^2(F_o{}^2)]^{1/2}/2F_o$ (p = 0.04). Intensities were considered as observed if $F_o{}^2 \geq 2.5\sigma(F_o{}^2)$, while F_o = 0.0 was given to the reflections having negative net intensities. The structure was solved by Patterson and Fourier methods and refined by full-matrix least squares. The function minimized was $[\sum w(\lvert F_o\rvert - 1/k\lvert F_c\rvert)^2]$ with $w = [\sigma^2(F_o)]^{-1}$. Anisotropic temperature factors were used for the Pd, P, and O atoms and for the carbon atoms of the cyclopentadienyl ring. Scattering factors were taken from the literature,[57] and the contribution of the real and imaginary part of the anomalous dispersion was taken into account.[57] The contribution of the hydrogen atoms in their calculated positions (C–H = 0.95 Å, B = 6.0 Å^2) was taken into account but not refined. Upon convergence (no parameter shift to esd ratio $>0.04\sigma(p)$) the Fourier difference map showed no significant features. All calculations were carried out by using the programs of the SDP package.[56] The handedness of the crystal was tested by refining the two possible sets of coordinates; those giving the lower R_w factor[58] are listed in Table VIII.

Table VIII. Final Positional Parameters for 4b

atom	x	y	z	B, Å^2
Pd	−0.23482 (6)	−0.06768 (5)	0.18229 (3)	3.203 (9)
P	−0.4105 (2)	0.0251 (2)	0.2306 (1)	3.36 (4)
O1	−0.3813 (6)	0.1716 (5)	0.2277 (3)	4.0 (1)
O2	−0.4563 (6)	0.0051 (6)	0.3042 (2)	4.1 (1)
O3	−0.5756 (6)	0.0120 (6)	0.2074 (3)	4.1 (1)
C1	−0.2560 (8)	0.2048 (7)	0.1918 (3)	3.5 (1)*
C2	−0.1705 (9)	0.1097 (8)	0.1687 (4)	3.5 (1)*
C3	−0.045 (1)	0.1421 (8)	0.1359 (4)	4.0 (2)*
C4	−0.014 (1)	0.2695 (9)	0.1269 (4)	4.6 (2)*
C5	−0.100 (1)	0.3609 (9)	0.1521 (5)	5.1 (2)*
C6	−0.2268 (9)	0.3286 (8)	0.1867 (4)	4.2 (1)*
C7	−0.3698 (9)	0.0063 (8)	0.3580 (4)	3.6 (1)*
C8	−0.2320 (9)	0.0592 (7)	0.3604 (4)	3.9 (1)*
C9	−0.156 (1)	0.059 (1)	0.4192 (4)	5.0 (2)*
C10	−0.215 (1)	0.004 (1)	0.4715 (4)	5.3 (2)*
C11	−0.348 (1)	−0.050 (1)	0.4686 (5)	5.9 (2)*
C12	−0.430 (1)	−0.0504 (9)	0.4114 (4)	4.7 (2)*
C13	−0.6100 (9)	0.0004 (7)	0.1407 (4)	3.7 (1)*
C14	−0.634 (1)	−0.114 (1)	0.1172 (5)	5.2 (2)*
C15	−0.681 (1)	−0.124 (1)	0.0524 (5)	6.1 (2)*
C16	−0.697 (1)	−0.022 (1)	0.0160 (5)	5.7 (2)*
C17	−0.672 (1)	0.090 (1)	0.0406 (6)	6.7 (3)*
C18	−0.628 (1)	0.106 (1)	0.1049 (5)	5.3 (2)*
C19	−0.127 (2)	−0.258 (1)	0.2085 (6)	9.3 (3)
C20	−0.257 (1)	−0.2788 (9)	0.1725 (5)	7.0 (3)
C21	−0.238 (1)	−0.235 (1)	0.1101 (5)	6.0 (2)
C22	−0.105 (1)	−0.180 (1)	0.1088 (4)	5.9 (2)
C23	−0.037 (1)	−0.194 (1)	0.1654 (6)	6.6 (2)

[a] Esd's are given in parentheses. Starred values denote refined isotropically; for those refined anisotropically B_{eq} values are given in the form $B_{eq} = {}^1/_3[a^2B_{11} + b^2B_{22} + c^2B_{33}]$.

Table IX

compd	solvent	reacn time, h	workup	yield, %
2a	toluene	5	RX; CH_2Cl_2/pentane	79
2b	toluene	5	RX; CH_2Cl_2/pentane	80
2c	toluene	5	RX; CH_2Cl_2/pentane	79
2c	p-xylene	1	RX; CH_2Cl_2/pentane	86
2d	toluene	5	oil	100
2d	p-xylene	1	oil	
2e	p-xylene	1	extraction with hexane gave pure prod.	90
2f	p-xylene	1	extraction with hexane gave pure prod.	96
2g	toluene[a]	3	suspension in pentane gave pure prod. as yellow powder	97
2h	toluene	3	suspension in pentane gave prod., which dec slowly	

[a] One hour in p-xylene affords decomposition.

Acknowledgment. A.A. thanks the CNR for support. P.S.P. thanks the ETH Zürich and the Swiss National

---

(56) *Enraf-Nonius Structure Determination Package*; Enraf-Nonius: Delft, Holland, 1986.

(57) *International Tables for X-ray Crystallography*; Kynock Press: Birmingham, England, 1974; Vol. IV.

(58) Hamilton, W. C. *Acta Crystallogr.* **1965**, *13*, 502.

(59) We cannot exclude adventitious H_2O.

(60) The data do not exclude an upfield shift due to ring formation.

Organometallics **1990,** *9,* 387–393

Science Foundation for support as well as the Johnson Matthey Research Centre, England for the loan of $PdCl_2$.

Registry No. **1a** (M = Pd), 38897-83-5; **1a** (M = Pt), 30053-58-8; **1b**, 42489-94-1; **1c**, 41944-80-3; **1d**, 41904-61-4; **1e**, 124379-82-4; **1f** (M = Pd), 124356-96-3; **1f** (M = Pt), 124356-97-4; **1g**, 124356-98-5; **1h**, 124356-99-6; **1i**, 74129-88-7; **2a** (X = Cl) (isomer I), 124357-00-2; **2a** (X = Cl) (isomer II), 124440-02-4; **2a** (X = I) (isomer I), 124357-21-7; **2a** (X = I) (isomer II), 124439-49-2; **2a** (M = Pt, X = Cl), 124379-84-6; **2b** (isomer I), 124439-40-3; **2b** (isomer II), 124439-41-4; **2c** (isomer I), 124357-01-3; **2c** (isomer II), 124439-42-5; **2d** (isomer I), 124440-01-3; **2d** (isomer II), 124357-19-3; **2e** (isomer I), 124357-02-4; **2e** (isomer II), 124440-03-5; **2f** (isomer I), 124357-03-5; **2f** (isomer II), 124439-43-6; **2g** (isomer I), 124357-04-6; **2g** (isomer II), 124439-44-7; **2h** (isomer I), 124357-05-7; **2h** (isomer II), 124439-46-9; **3a**, 124357-06-8; **3b**, 41871-86-7; **3c**, 124357-07-9; **3d** (isomer I), 124357-08-0; **3d** (isomer II), 124439-45-8; **3e**, 124357-09-1; **3f**, 124357-10-4; **3g**, 124357-11-5; **3h** (isomer I), 124357-12-6; **3h** (isomer II), 124439-48-1; **3i** (isomer I), 124357-13-7; **3i** (isomer II), 124439-47-0; **3k**, 124357-20-6; **3l**, 124357-14-8; **4a**, 124357-15-9; **4b**, 124357-16-0; **4c**, 124357-18-2; **5a**, 124379-83-5; **5b**, 124399-59-3; $PdCl_2$, 7647-10-1; $PdCl_2(PhCN)_2$, 14220-64-5; $PtCl_2$, 10025-65-7.

Supplementary Material Available: Positional parameters and their estimated standard deviations (Table S1), general temperature factor expressions (Table S2), bond distances (Table S3), and bond angles (Table S4) (6 pages); observed and calculated structure factors (Table S5) (18 pages). Ordering information is given on any current masthead page.

Formation of Cationic MPt Heterobimetallic μ-Phosphido μ-Hydrido Complexes

John Powell,* Eric Fuchs, Michael R. Gregg, Jacqueline Phillips, and Matthew V. R. Stainer

Department of Chemistry, University of Toronto, Toronto, Ontario, Canada M5S 1A1

Received June 9, 1989

The cationic secondary phosphine complexes $[CpM(CO)(L)(PR_2H)]^+X^-$ (M = Ru, PR_2H = PPh_2H, $PPhH_2$, L = CO; M = Fe, PR_2H = PPh_2H, L = CO, MeC≡CMe, C_2H_4; M = Mn PR_2H = PCy_2H, PPr_2H, L = NO; X^- = BF_4^-, PF_6^-) and $[(\eta^7\text{-}C_7H_7)(CO)_2Mo(PCy_2H)]PF_6$, prepared by following literature procedures for the synthesis of their PPh_3 analogues, react with $Pt(C_2H_4)(PPh_3)_2$ to give $[Cp(L)M(\mu\text{-}PR_2)(\mu\text{-}H)Pt(PPh_3)_2]X$ and $[(\eta^7\text{-}C_7H_7)(CO)Mo(\mu\text{-}PCy_2)(\mu\text{-}H)Pt(PPh_3)_2]X$ as the final products. The reactions proceed by one or both, of two possible reaction pathways. One pathway involves the initial oxidative addition of a P–H bond to the Pt(0) complex to give $[Cp(CO)LM(\mu\text{-}PR_2)PtH(PPh_3)_2]X$ followed by PPh_3 loss from Pt and CO transfer from M to Pt (via a bridging CO). The rate of this CO-transfer step is sterically driven, in a manner similar to that observed for ortho-metalation reactions, with observed relative rates being as follows: μ-PPh_2 ≫ μ-PPhH; μ-PCy_2 > μ-PPr_2; μ-PPh_2 ≫ μ-$AsPh_2$; Cr > Mo > W; Fe > Ru; Mn ≫ Re; $\eta^5\text{-}C_5H_4Me > \eta^5\text{-}C_5H_5$. The more acidic (P–H) secondary phosphine complexes react with Pt(0) complexes by a route that involves deprotonation of the coordinated secondary phosphine to give a phosphidometal complex, which then substitutes a ligand from Pt(0) followed by CO transfer to Pt. Reprotonation of the resultant complex gives $[Cp(L)M(H)(\mu\text{-}PR_2)Pt(CO)(PR_3)]^+$ (PR_3 = PPh_3). Several complexes of this type (PR_3 = PCy_3) were prepared and studied from the reaction of $[CpM(CO)(L)(PR_2H)]^+$ with $Pt(C_2H_4)_2(PCy_3)$. The deprotonation pathway provides for faster Pt-assisted CO labilization/loss than the P–H oxidative-addition route. The ${}^1J_{^{195}Pt-^{31}P_\mu}$ coupling constants for a series of bimetallic μ-phosphido μ-hydrido complexes of the type $[M](\mu\text{-}PPh_2)(\mu\text{-}H)Pt(PPh_3)_2^+$ are shown to be much more sensitive to structural changes than the ${}^1J_{^{195}Pt-^{31}P}$ values of the PPh_3 trans to P_μ. While a plot of individual ${}^1J_{^{195}Pt-^{31}P}$ vs ${}^1J_{^{195}Pt-^{1}H}$ values gives relatively poor correlations, a plot of $\sum {}^1J_{^{195}Pt-^{31}P}$ (all three ^{31}P nuclei) vs ${}^1J_{^{195}Pt-^{1}H}$ is considerably improved suggesting an overall self-compensating effect for distortions/structural changes in individual Pt–P bonds as [M] is varied. For these structurally very similar complexes ${}^2J_{^{31}P_\mu-^{31}P}$(trans) varies almost linearly with ${}^1J_{^{195}Pt-^{31}P_\mu} + {}^1J_{^{195}Pt-^{31}P}$(trans to P_μ).

Introduction

Oxidative addition of the P–H bond of a secondary phosphine complex to zerovalent complexes of platinum provides easy access to singly bridged μ-phosphido heterobimetallic hydrides.[1-5] For example the metal carbonyl complexes $M(CO)_5(PPh_2H)$ (**1**; M = Cr, Mo, W) oxidatively add to $Pt(C_2H_4)(PPh_3)_2$ to give the μ-phosphido bimetallic $(OC)_5M(\mu\text{-}PPh_2)PtH(PPh_3)_2$ (**2**).[1] This complex loses CO under very mild conditions (for a group VI carbonyl)[6] to give the μ-phosphido μ-hydrido complex $(OC)_4M(\mu\text{-}PPh_2)(\mu\text{-}H)Pt(PPh_3)_2$ (**3**; eq 1). While the net result of

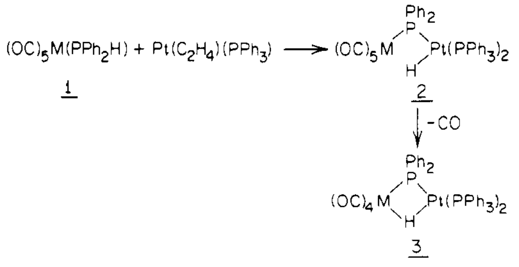

(1)

this reaction is effectively a substitution of CO at M by H, the reaction proceeds by a platinum-assisted process involving PPh_3 dissociation and a CO transfer, via a μ-CO intermediate, from M to Pt as outlined in Scheme I, route 1. Both the rate and the nature of the reaction of secondary phosphine complexes with Pt(0) systems are sen-

---

(1) Powell, J.; Gregg, M. R.; Sawyer, J. F. *Inorg. Chem. 1989, 28,* 4451.

(2) Powell, J.; Sawyer, J. F.; Stainer, M. V. R. *Inorg. Chem.* **1989,** *28,* 4461.

(3) Powell, J.; Sawyer, J. F.; Smith, S. J. *J. Chem. Soc., Chem. Commun.* **1985,** 1312.

(4) Powell, J.; Gregg, M. R.; Sawyer, J.. *J. Chem. Soc., Chem. Commun.* **1987,** 1029.

(5) Schwald, J.; Peringer, P. *J. Organomet. Chem.* **1987,** *323,* C51.

(6) Reger, D. L.; Belmore, K. A.; Mintz, E.; McElligott, P. J. *Organometallics* **1984,** *3,* 134.